RSC Advances




ROYAL SOCIETY OF CHEMISTRY

www.rsc.org/advances

Journal Name

ARTICLE

# Well-dispersive graphene-polydopamine-Pd hybrid with enhanced catalytic performance

Jian-Xin Ma, Honglei Yang, Shuwen Li, Ren Ren, Jing Li, Xueyao Zhang and Jiantai Ma*

Received 00th January 20xx,
Accepted 00th January 20xx

DOI: 10.1039/x0xx00000x

www.rsc.org/

Inspired by the discovery of the adhesive proteins in mussels' clues, we prepared a graphene-polydopamine (GPDA) hybrid, in which the commonly used graphene oxide was replaced by graphene synthesized through physical routes. Then the ultrafine Pd nanoparticles were decorated on the hybrid to obtain a stable and well-dispersed catalyst in polar solvents. The Pd nanoparticles on graphene-polydopamine (GPDAP) were 2.0 nm in average and processed a good monodispersibility on the polydopamine modified graphene, while the size of the Pd particles on unmodified graphene (GP) was larger than 4.0 nm and obviously aggregated. The catalytic activity of the catalyst was investigated in the reduction of 4-nitrophenol (4-NP), $K_3[Fe(CN)_6]$, methylene blue (MB) and rhodamine B (RhB), respectively, which are common industrial pollutants. The comparison between Pd/C (CP) and GP, GPDA prevailed that the prepared catalyst GPDAP showed superior activity even just tiny amount of catalyst was added.

## 1 Introduction

Dyes, which are widely used in many industries, cause serious environmental pollution, due to their toxicity and difficulty to degrade. As a kind of dye used in pesticides, dyeing, pharmaceutical industry, 4-nitrophenol (4-NP) is produced in the highest quantities among phenol derivatives in the world[1]. For sake of the existence of the nitro group, the ring of the 4-NP is further stabilized, which makes it hard to degrade in the natural environment. Other dyes like methylene blue (MB) and rhodamine B (RhB) are also carcinogenic and difficult to degrade.

Due to their toxicity and stability, many efficient catalysts such as noble metals are frequently used for the disposal of dyes[2]. Currently, a cheaper noble metal Pd showed much higher activity for the catalytic oxidation, catalytic hydrogenation, cross-coupling reactions [3-5], and reduction of 4-NP compared to other commonly studied noble metals [6]. For example, Zhang *et al.* reported the development of a new type of bifunctional nanocatalyst based on three-dimensional macroscopic carbon nanotube-graphene hydrogel supported Pd nanoparticles and explored its practical application in catalytic reduction of p-nitrophenol [7]. In 2013, a kind of ultrafine Pd nanoparticles was prepared, which was encapsulated by Double-shelled hollow carbon spheres with reduced graphene oxide as inner shell and carbon layer as outer shell and it exhibited superior performance in the reduction of p-nitrophenol [8]. Moreover, improving the surface area and the quantity of steps and kinks on the surface can enhance the catalytic activity of the metallic nanoparticles. Based on the above properties, smaller size of the metal particle is beneficial for the activities of the catalysts. However, serious aggregation makes it hard to prepare small and monodispersed particles. To avoid the aggregation, different kinds of supports, such as $Al_2O_3$, MOF and graphene, have been used to minimize the total surface energy and stabilize the nanoparticles [9-13].

Graphene, a kind of marvelous two-dimensional carbon nanosheets, with a structure of honeycomb, has attracted great attention because of its high strength and excellent conductivity to both heat and electricity. Since discovered by Novoselov *et al* in 2004 [14], graphene has been applied in many fields, such as transistors [15], biosensors [16], fuel cells [17], catalysts [18, 19], hydrogen storage [20], and drug delivery [21]. As a support of catalyst, it can stabilize nanoparticles through static interaction, as well as improve the catalytic performance through synergistic interaction between nanoparticles and graphene [22]. Though the excessive charge makes pure graphene a good support to stabilize nanoparticles, the static interaction is not strong enough to prevent the aggregation effectively [23]. In order to solve this problem, the functionalization of graphene *via* covalent or noncovalent method is considerably investigated. The covalent functionalization shows strong bond intensity. Yet, the extended aromatic structure of graphene is perturbed, just because of binding to or generating defects on graphene [24-26]. Compared to covalent, noncovalent functionalization can attach functional groups to graphene without disturbing the aromatic structure [27, 28]. In most cases, the strength of this kind of decoration is not as intense as that of covalent decoration. Therefore, it is crucial to find out an approach combining advantages of both covalent and noncovalent functionalization.

*State Key Laboratory of Applied Organic Chemistry, Gansu Provincial Engineering Laboratory for Chemical Catalysis, College of Chemistry and Chemical Engineering, Lanzhou University, Lanzhou 730000, PR China*

E-mail: majiantai@lzu.edu.cn; Fax: +86-931-8912582; Tel: +86-931-8912577

Electronic Supplementary Information (ESI) available. See DOI: 10.1039/x0xx00000x

Recently, polymers with aromatic structures have been employed to functionalize graphene [29, 30]. The discovery of adhesive proteins in mussels' clues, which are rich in 3,4-dihydroxy-L-phenylalanine as the main role to interact with substrates [31], propelled a new strategy of surfaces modification. Inspired by this versatile adhesives of invertebrate mussels, in 2007, Lee *et al*. [32] reported a method to functionally modify material surfaces with polydopamine (PDA), a kind of structure similar to DOPA, interacting with surfaces by intensive covalent and noncovalent binding[33]. For this reason, PDA is a promising alternative to functionalize graphene which combines advantages of both covalent and noncovalent functionalization. Xu *et al*. reduced GO with dopamine to obtain polydopamine functionalized reduced graphene oxide (rGO) [34]. Ye *et al.* designed a route to synthesize a polydopamine (PDA)-Ag-reduced graphene oxide (RGO) hybrid and hybrid was applied to the oxidation of hydroquinone to benzoquinone in the presence of $H_2O_2$ [35]. Furthermore they synthesized flowerlike Pt nanocrystals on poly-dopamine (PDA) functionalized reduced oxide graphene (RGO) [36]. The Pt(F)-PDA/RGO catalyst showed improved catalytic activity and stability toward methanol electrooxidation. Zhao *et al.* immobilized $Cu^{2+}$ on magnetic graphene@polydopamine (magG@PDA@$Cu^{2+}$) composites and applied the novel nanocomposites to the enrichment and identification of low-concentration standard peptides [37]. However, strong oxidizer and concentrated acid are needed to prepare GO, which consumes a large quantity of dangerous reagent and produces environmental pollutants. Paton *et al*.[38] exfoliated graphite in solution to prepare graphene large-scale directly, which means graphene prepare with physical route could be more available and cheaper than traditional GO in the near future. But fewer -OH and -COOH on it than GO made it hard to disperse in polar solvent without the aid of surfactants. To mimic the directly exfoliated graphene, we chose commercialized graphene prepared through physical route which is also short of -OH and -COOH to proceed the experiment.

Based on the reasons above, we functionalized graphene synthesized through physical routes, instead of traditional GO, with polydopamine through self-polymerization of dopamine directly, which is facile and more useful for large scale preparation in the future. Furthermore, ultrafine Pd nanoparticles were decorated on graphene-polydopamine (GPDA) hybrid with simple method with no surfactant added. To evaluate the catalytic activity of our catalyst, it was used in the reduction of 4-NP and $K_3[Fe(CN)_6]$ by borohydride ions compared with commercial grade palladium on carbon (CP) and graphene-Pd (GP) prepared with similar process to that of graphene-PDA-Pd (GPDAP) [39]. Further application of two famous dyes (MB and RhB) for degradation was studied. The processes were recorded in situ by UV-VIS spectrophotometer.

## 2 Experimental

### 2.1 Materials

Graphene (Diameter: 0.5~2 μm, Thickness: ~0.8 nm, Single Layer Ratio: ~80%, Purity: ~99%, BET surface area (m2/g): 500~1000, Electrical resistivity (Ω.cm): ≦0.30) prepared by physical method was purchased from Nanjing XFNano Material Tech Co., Ltd., Dopamine was purchased from Energy Chemical of Sun Chemical Technology (Shanghai) Co., Ltd., Tris (99.8%) was purchased from Pengcheng Biological Technology Development Co., Ltd., $K_2PdCl_4$ (99.9%) was purchased from J&K Scientific Ltd., KCl was purchased from Cheng Du Ke Long Chemical Co., Ltd., $NaBH_4$ was purchased from Sinopharm Chemical reagent Co., Ltd., Ethenol was purchased from Rionlon Development Co., Ltd.

### 2.2 Preparation of Graphene-PDA (GPDA)

HCl (5 M) was added to the solution of Tris to obtain 10 mM Tris-Cl buffer (pH=8.5) and 50 mg of dopamine hydrochloride was dissolved in 10 mL DI water. Subsequently, 50 mg Graphene was added to 100 mL Tris-Cl buffer and the solution was sonicated for 30 min in an ice-salt bath. The suspension was stirred vigorously for 10 min. Then 5 mL dopamine hydrochloride was added to the flask. The reaction was stirred at 60 ℃ for 24 hours. In the end, the product was filtrated with 400 nm nanofiltration membrane, washed by water and alcohol for several times and dried reduced pressure at 60 ℃ overnight. Black powders were obtained.

### 2.3 Preparation of Graphene-PDA-Pd (GPDAP)

20 mg GPDA was dispersed in 40 mL DI water and sonicated for 30 min, followed by adding 3.77mL $K_2PdCl_4$ (5 mM) and keeping stirring for 1 h. After that 40mL $NaBH_4$ (2.5mM) was added dropwise in 30 min. After being stirred for 3 h, the product was obtained by filtration, thoroughly rinsed with water and alcohol and dried in reduced pressure desiccator for 24h.

### 2.4 Preparation of Graphene-Pd (GP)

20 mg graphene was dispersed in 40 mL DI water. Then 3.77mL $K_2PdCl_4$ (5mM) was added and kept stirring for 1 h. After that, GP was prepared similarly to the former process.

### 2.5 Characterization

The structure of our catalyst was analyzed with Raman spectrometer (inViaRenishaw confocal spectrometer with 633 nm laser excitation). The morphology, size, and size distributions of the Pd particles were investigated using transmission electron microscopy (TEM, Tecnai G2 F30 electron microscope operating at 300 kV). X-ray diffraction (XRD) measurements were carried out with a high-resolution X-ray diffractometer (Rigaku D/max2400 diffractometer). The concentration of Pd in our catalyst was analyzed using inductive coupled plasma atomic emission spectrometer (ICP-AES), which was conducted with PerkinElmer (Optima-4300DV). The reaction was investigated with UV-VIS absorption spectra (HP/Agilent 8453 UV/Vis Spectrophotometer).

### 2.6 Catalytic reduction of 4-nitrophenol

200 μL of 4-notriphenol (1 mM) was mixed with 1.2mM DI water and 1.5 mL of fresh $NaBH_4$ (10 mM) solution in a quartz cuvette. And 1 mg catalyst was dispersed into 10 mL DI water. As soon as 100 μL catalyst solution was added, monitoring the

reaction with UV-VIS spectroscopy at 25 ℃. And the kinetics was measured at a wavelength of 400 nm.

### 2.7 Catalytic reduction of hexacyanoferrate (III)

200 μL of hexacyanoferrate (III) (10 mM) was mixed with 1.25mL DI water and 1.5 mL of fresh $NaBH_4$ (10 mM). After that, 50 μL catalyst solution (0.1 mg/mL) was added. the catalytic reduction of dyes, time-dependent absorption spectra were recorded at 15 ℃.

### 2.8 Catalytic degradation of organic dyes

1 mg of catalyst was ultrasonically dispersed in 10 mL DI water. Then 10 μL catalyst solution was added to 50 μL MB (2 mM) solution, followed by the addition of 1.5 mL freshly prepared $NaBH_4$ solution (10 mM). 1.45mL DI water was added to keep the reaction system in proper concentration. The extent of the reaction was monitored by UV-VIS spectrophotometer in situ. The degradation of RhB was studied under same condition, except the quantity of catalyst solution was 50 μL.

## 3 Result and discussion

Inspired by the fabulous adherence of mussels, we designed a simple method for functionalization of pure graphene. The chelation of Pd(II) ions on catechol structure leads to good monodispersity of reduced Pd nanoparticles and that kind of strong interaction can prevent particles from aggregation, as illustrated in the Fig.1. Furthermore, the coordination of amino groups to Pd is also strong to improve the stability [40, 41]. And dispersibility of our catalyst was highly boosted. It is believed that the mussel-inspired polydopamine decoration have a promising future. The contents of nitrogen in graphene-PDA hybrid was 2.4 wt% characterized by ICP-AES. Therefore, the percentage of PDA in GPDA was 26.25%. Furthermore, 7.9wt% of Pd was disposed on GPDA in GPDAP and 7.3wt% was disposed on graphene in GP, indicated by the ICP-AES analysis. The content of Pd in GPDAP was higher than GP even excessive $NaBH_4$ added, due to the coordination of Pd ions with catechol structures and amino groups.

Fig.2 showed Raman spectra of Graphene, polydopamine and Graphene-PDA hybrid (GPDA). In the spectrum of graphene, there were two strong featured bands, the vibrational D band at 1350 $cm^{-1}$ and the G band at 1580 $cm^{-1}$. D band arose from the defects at the edge of graphene and interaction with the substrate [42]. Polydopamine also showed two broad bands at 1350 $cm^{-1}$, 1580 $cm^{-1}$, coming from vibration of aromatic rings and aliphatic C-C and C-O stretching[43]. The sum of two constitutions was observed in GPDA. The ratios of intensity of peaks ($I_D/I_G$) before and after the modification were calculated, which changed from 1.46 to 1.18 after PDA modified, inferring the less defects after decoration with PDA. That is because the defects on graphene was covered by polydopamine which also possesses aromatic structures [44].

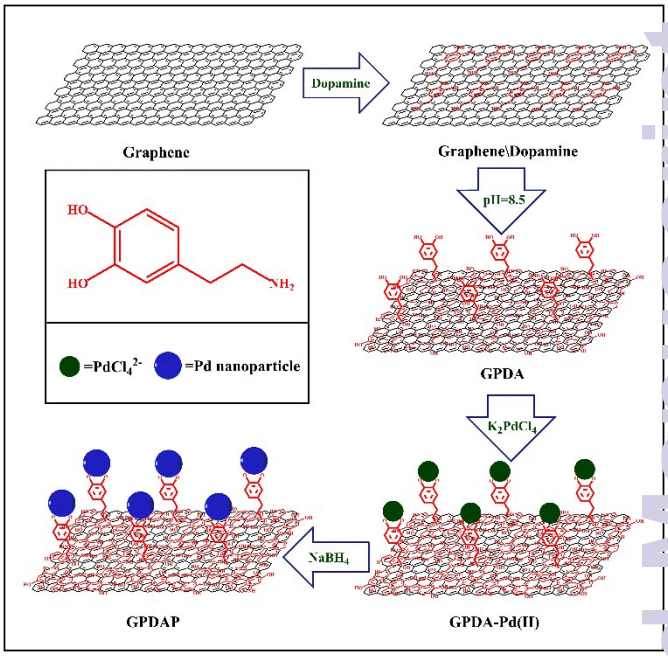


Fig.1 Schematic illustration for the preparation of GPDAP.

The TEM of GPDAP compared with Graphene Pd were given in Fig.3. The fabulous feature was that the Pd particles on GPDA were monodispersed and well-distributed, while the size of Pd without PDA not was as homogenous as the former. The high resolution TEM (HRTEM) obviously visualized the aggregation of Pd without PDA and good monodispersity when PDA was added. By statistical analyzing the particle size distribution, as seen in the inserts of Fig.3 (A) and (B),the mean particle size of Pd in GPDAP was 2.0 nm and processed bett monodispersibility, most of which distributed in a narrow range from 1 to 3 nm. However, the diameter of Pd nanoparticles in GP was as large as 4.5 nm in average and disperses from 1 to 9 nm. This could be ascribed to catechol and amino groups stabilizing the particles and lowing the energy [41]. In the image of HRTEM, the interplanar spacing of Pd lattice could be distinguished clearly to be 0.226 nm, which matched well with the (111) lattice of spacing of Pd (0.225 nm) [45]. Based on the results of TEM, GPDAP had a larger surface area and more Pd atoms were exposed.

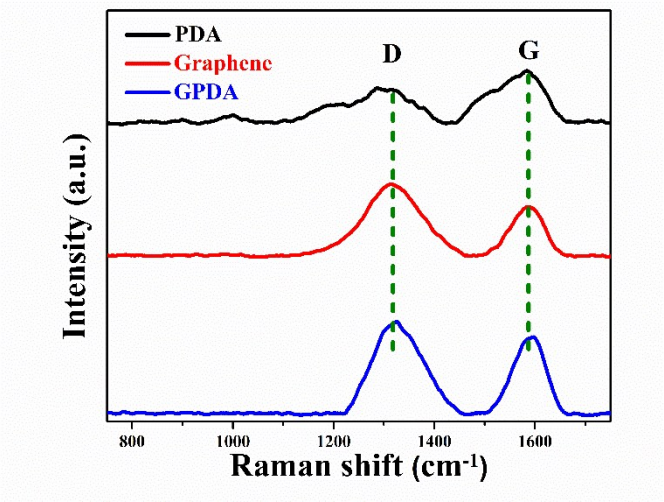


Fig.2 Raman spectra of PDA, graphene and GPDA.

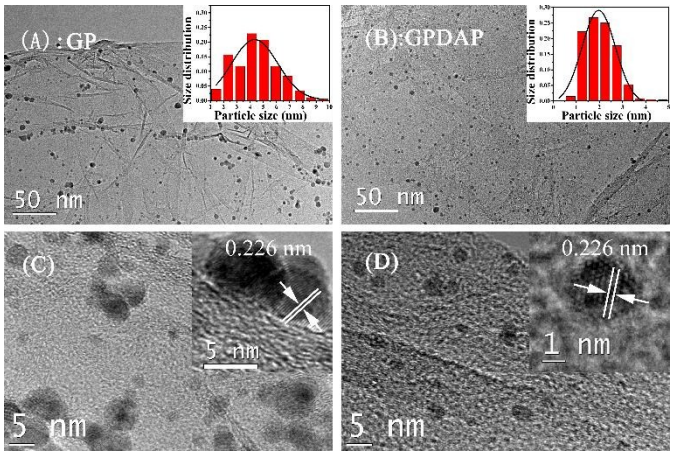


Fig.3 TEM image of GP (A and C) and GPDAP (B and D). Insert: particle size distribution graphs of Pd nanoparticles in GP (A) and GPDAP (B) and HRTEM of GP (C) and GPDAP (D).

XRD was measured to study the structure of our catalysts. In consideration of the GP, the peaks in the Fig.4 demonstrated the existence of both Graphite-like crystalline and Pd particles. The broad diffraction peak at 26.3 °came from the (002) crystal face of graphene. The other four peaks at 40.4 °, 46.8 °, 68.4 °and 82.4 ° corresponded to the (111), (200), (220) and (311) crystalline plane of Pd particles [46]. For GPDAP, similar features were presented. The average particle size of Pd in GPDAP calculated from the Pd (111) peak according to the Scherrer's Formula was 2.1 nm, which agreed well with the TEM result. The XRD result confirmed the Pd particle was successfully immobilized on graphene-polydopamine hybrid.

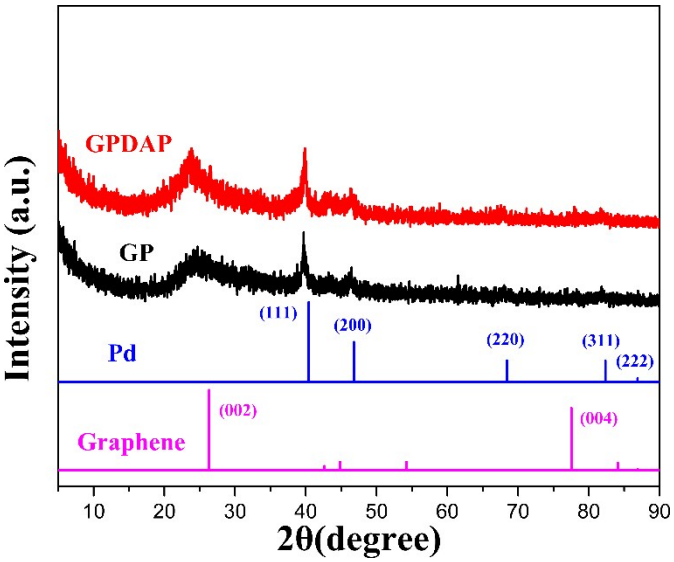


Fig.4 XRD spectra of GPDAP, GP and the standard bar graph of Pd and pure graphene.

Typical XPS spectra of GP and GPDAP were depicted in Fig. 5. The existence of N 1s (400.8eV) further confirmed that the graphene was decorated by PDA through π-π interaction. Peaks at 335.4 eV which was for $3d_{5/2}$ of Pd nanoparticles indicated the existence of Pd in our catalysts [41, 47]. Comparing the high resolution XPS spectra of Pd in GPDAP with that in GP, the peak of Pd $3d_{5/2}$ of GP is 335.51 eV and that of GPDAP is 337.95 eV. An obvious shift of 2.44 eV was recognized after the decoration of PDA, which may due to the strong interaction between amino group or catechol structure and Pd nanoparticles.

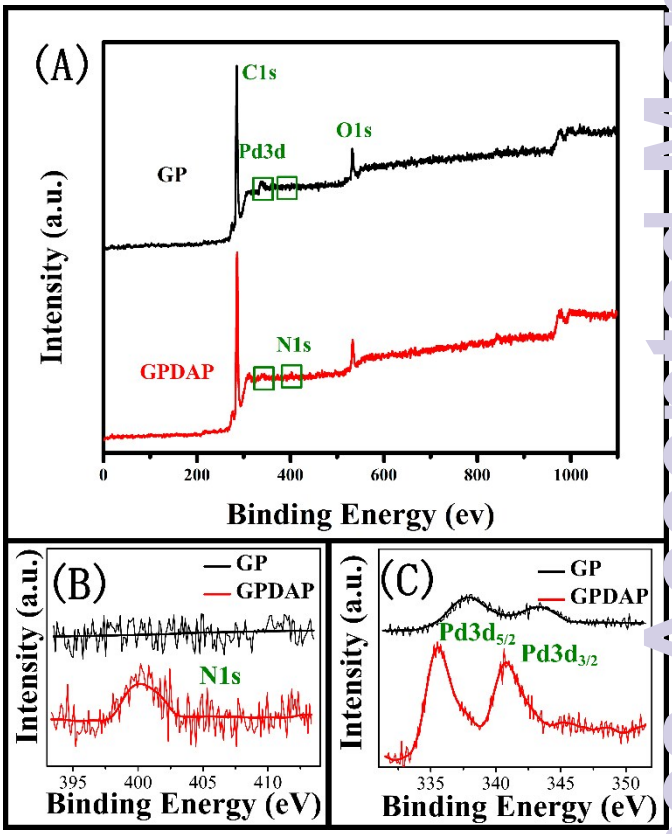


Fig. 5 (A) XPS wide-scan spectra of GPDAP and GP. (B) N 1s core level spectra of GPDAP and GP. (C) Pd 3d core level spectra of GPDAP and GP

For heterogeneous catalysts, the dispersibility in solution plays a key role in the activity of catalysis. Based on the properties of hydroxyl groups on the surface, our catalyst showed fabulous dispersibility. Catalysts with and without polydopamine added were compared. As shown in Fig.6, the photos were taken after 0 h (A), 2 h (B), 5 h (C) and 7 h (D). The concentrations of both solution are 0.5mg/mL and the solution started to precipitate after 7 days. Obviously, the dispersibility of GPDAP was well improved by polydopamine.

So as to accurately demonstrated catalytic ability of our catalyst, our catalysts (GPDAP, GP and CP) were used in two widely used catalytic model reactions [39, 48], *viz.* the reduction of 4-NP by sodium borohydride and the reduction of ferrocyanate(III) [49],as shown in Fig.6 (E).

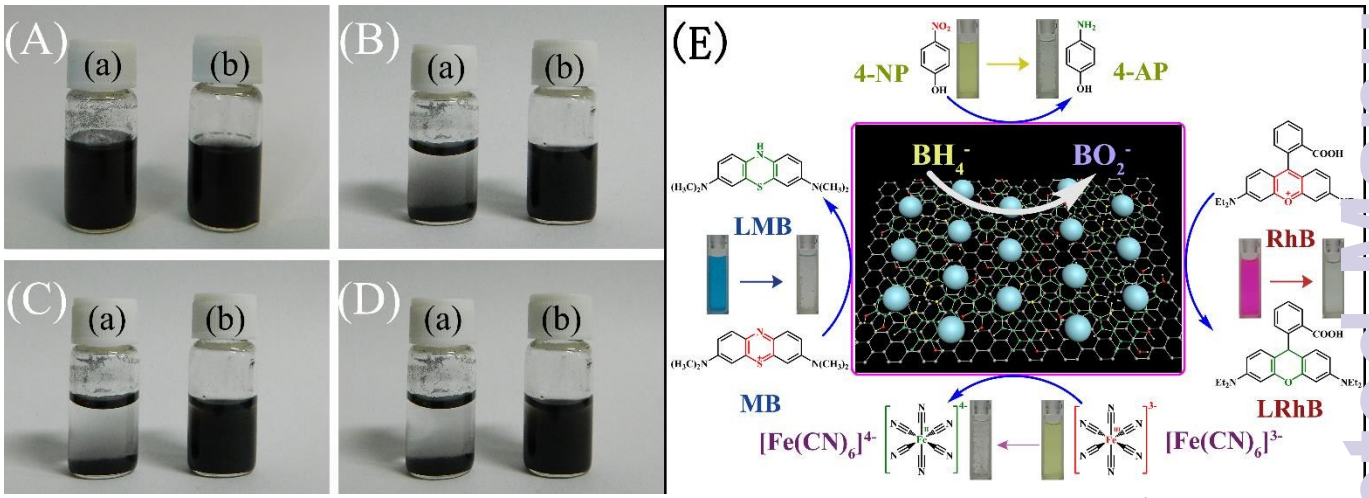


Fig.6 Photographs of (a) GP and of (b) GPDAP dispersed in DI water after 0 h(A), 2 h (B), 5 h (C) and 7 h (D). the concentration of both solution is 0.5 mg/mL. (E) The illustration of the reduction of 4-NP, $K_3[Fe(CN)_6]$, RhB and MB catalyzed by GPDAP.

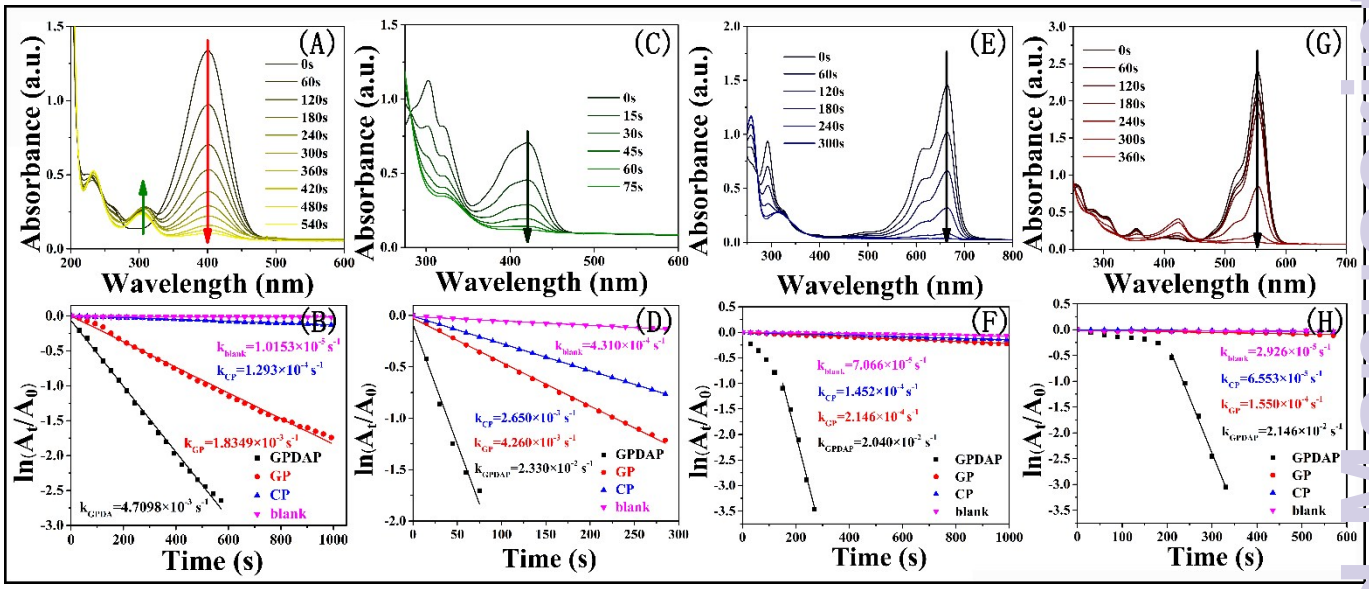


Fig. 7 UV-visible absorption spectra of the reduction of 4-NP (A), $K_3[Fe(CN)_6]$ (C), MB (E), RhB (G) catalysed by GPDAP. Plot of ln(Ct/C0) versus time spectra for the reduction of 4-NP (B), $K_3[Fe(CN)_6]$ (D), MB (F), RhB (H) catalyzed by GPDAP, GP, CP and nothing added.

When studying the former model reaction, the extent of reactions was monitored in situ by measuring the UV-VIS absorption spectra of the reactant mixture to ensure the precision of surveillance, because the reaction was so fast that to separate the products in such short time was infeasible. A peak of the reactant 4-NP was showed at 400 nm and that of the product 4-aminophenol (4-AP) at 315 nm [50].

Initially, a blank experiment was tried, during which no catalyst was added. The 4-NP solution showed yellowish, while it turned dark yellow after $NaBH_4$ was added. After that, the peak of 4-NP at 400 nm remained unchanged. That indicated that it can't react in the absence of catalysts. Then with catalysts (GPDAP, GP and CP) added in other experiments, the intensity of the peak of 4-NP at 400 nm decreased as the reaction extended and a new peak of 4-AP appeared gradually at 315 nm. An interesting phenomenon was observed that the peak at 315 nm did not always increase as the 4-NP was reduced. The abnormality might be attributed to the absorption of products on graphene [51, 52], or cumulation of intermediates [53].

When 10 μL GPDAP was added, the intensity of absorption at 400 nm decreases sharply and the system turned transparent within 600 s, as Fig.7 (A) showed. However, the other catalyzed with GP became yellowish after 1000 s (Fig. s2). And we also tried one with CP, the colour of which remained almost unchanged owing to low quantities of catalysts. Only in the spectra can we distinct the decrease of the peak at 400 nm.

The concentration of the $BH_4^-$ exceeded 100 times than that of 4-NP and catalysts, so we could ignore the degradation of $BH_4^-$ ions and treated the concentration of $BH_4^-$ as constant. Furthermore, since the concentration of $NaBH_4$ was so high that we could treat the reduction as pseudo-first-order with respect to the concentration of 4-NP [54, 55]. That is, $ln(A/A_0)$ and time shows good linear relationship, so we can write the kinetic equation for the reaction as follows:

$$\frac{dC_t}{dt} = \frac{dA}{dt} = \ln\left(\frac{C_t}{C_0}\right) = \ln\left(\frac{A_t}{A_0}\right) = -kt$$

Where, $C_t$ and $C_0$ are the concentration of 4-NP at time t and the start separately. $A$ in the equation stands for the absorption of 4-NP. As seen in the Fig.7(B), the rate constants $k$ calculated from the slopes was $4.7098\times10^{-3}$ $s^{-1}$, $1.8349\times10^{-3}$ $s^{-1}$, $1.2937\times10^{-4}$ $s^{-1}$ and $1.0153\times10^{5}$ $s^{-1}$ attributed to GPDAP, GP, CP and no catalyst added respectively. The content of Pd in our catalyst (GPDAP 7.9%, GP 7.3% and CP 10%) was analyzed using ICP-AES. To compare with the activity of catalysts in literatures reported before, a factor $k^*$ defined as the rate constant over the weight of catalyst ($k^*=k/m$) was calculated. Then we got $k^*$(GPDAP)$=4.7098\times10^{2}$ $s^{-1}g^{-1}$, $k^*$(GP)$=1.8349\times10^{2}$ $s^{-1}g^{-1}$ and $k^*$(CP)$=12.937$ $s^{-1}g^{-1}$. Compared with k* of catalyst reported in literatures in Table s1, our catalyst showed higher activity. The excellent activity of GPDAP probably came from (1) better dispersibility developed by hydroxyl of polydopamine (Fig.6), (2) good monodispersity and smaller size of Pd which means larger active surface (Fig.3) and (3) π-π interaction between graphene and aromatic reactant to highly improve the concentration of 4-NP on the surface of catalysts [22].

Another famous reaction we used was the reduction of hexacyanoferrate (III) by borohydride. What is interesting of this reaction is both states of the ions are stable and possess the same chemical composition. Because of these particularities, no induction period, which was often observed in reduction of organic dyes such as 4-NP reduction, had been observed in this

reaction, as shown in Fig.7 (C). Like the former reaction, the reduction of hexacyanoferrate (III) was carried out on condition that the $BH_4^-$ was far more excessive than $[Fe(CN)_6]^{3-}$ to minimalize the influence of the concentration of $BH_4^-$ and to inhabit the hydrolysis of $BH_4^-$. The rate of reaction was monitored *in situ* by spectrophotometer with the decrease of the absorption at 420 nm. Interestingly, the presence of the catalysts changed the order of the reaction, as reported, from zero order kinetics to first order kinetics [49]. In order to compare the rates before and after the addition of the catalysts and to simplify the experiment, we treated the reaction with no catalyst added as a first order reaction, which did not affect the result of the experiment.

The rate constants for the reductions were $k$(GPDAP)=2.330×10$^{-2}$ s$^{-1}$, $k$(GP)=4.260×10$^{-3}$ s$^{-1}$ and $k$(CP)=2.650×10$^{-3}$ s$^{-1}$, as the Fig.7 (C, D), and factor $k$* was calculated ($k$*(GPDAP)=4.660×10$^{3}$ s$^{-1}$g$^{-1}$, $k$*(GP)=8.520×10$^{2}$ s$^{-1}$g$^{-1}$ and $k$*(CP)=5.300×10$^{2}$ s$^{-1}$g$^{-1}$) that indicated the catalyst GPDAP showed higher catalytic activity than the GP and CP. The remarkably high activity may come from the high accessible surface area of the ultrafine Pd nanoparticles.

For further application of the catalyst, we applied our catalyst GPDAP in the reductive degradation of two major toxics in many industries, MB and RhB, as Fig.7(E-H) showed, compared with GP, CP and no catalyst was added.

First, reductive degradation of MB was studied. The absorption band appeared at 665 nm corresponded to the n-π* transition of MB and the MB was reduced to leuco methylene blue (LMB) [55-57]. For reason of the excessive $BH_4^-$, the reactions were also treated as first order reaction and the ratios of $ln(A_t/A_0)$ to time were calculated as shown in Fig.7 (F). The ratio of the reaction without catalysts is $k$(blank)=7.066×10$^{-5}$ s$^{-1}$. The reaction proceeded faster after adding GP and CP. To our surprise, by adding GPDAP, the reduction was greatly enhanced ($k$(GPDAP)=2.040×10$^{-2}$ s$^{-1}$). The degradation of MB to LMB was accomplished in less than 300 s in the presence of ultrafine Pd catalysts, GPDAP. An inductive time of about 150 s was observed during the reduction, owing to surface restructuring of the catalyst [58, 59].

**Table 1** Summary of the constants for the catalytic reductions

| Catalyst | Substance | $k$ (s$^{-1}$) | Catalyst dosing | $k$* (s$^{-1}$g$^{-1}$) |
|---|---|---|---|---|
| GPDAP | 4-NP | 4.7098×10$^{-3}$ | 10 μg | 4.7098×10$^{2}$ |
| GP | 4-NP | 1.8349×10$^{-3}$ | 10 μg | 1.8349×10$^{2}$ |
| CP | 4-NP | 1.2937×10$^{-4}$ | 10 μg | 12.937 |
| None | 4-NP | 1.0153×10$^{-5}$ | - | - |
| GPDAP | $K_3[Fe(CN)_6]$ | 2.330×10$^{-2}$ | 5 μg | 4.660×10$^{3}$ |
| GP | $K_3[Fe(CN)_6]$ | 4.260×10$^{-3}$ | 5 μg | 8.520×10$^{2}$ |
| CP | $K_3[Fe(CN)_6]$ | 2.650×10$^{-3}$ | 5 μg | 5.300×10$^{2}$ |
| None | $K_3[Fe(CN)_6]$ | 4.310×10$^{-4}$ | - | - |
| GPDAP | MB | 2.146×10$^{-2}$ | 1 μg | 2.146×10$^{4}$ |
| GP | MB | 1.550×10$^{-4}$ | 1 μg | 1.550×10$^{2}$ |
| CP | MB | 6.553×10$^{-5}$ | 1 μg | 65.53 |
| None | MB | 2.926×10$^{-5}$ | - | - |
| GPDAP | RhB | 2.040×10$^{-2}$ | 5 μg | 4.080×10$^{3}$ |
| GP | RhB | 2.146×10$^{-4}$ | 5 μg | 42.92 |
| CP | RhB | 1.452×10$^{-4}$ | 5 μg | 29.04 |
| None | RhB | 7.066×10$^{-5}$ | - | - |

The reduction degradation of another organic toxic RhB to leuco Rh B (LRhB) which had often been used as fluorescence dye was then studied [60, 61]. The ratios of $ln(A_t/A_0)$ to time were calculated and the result was similar to that of MB. The activity of catalyst GPDAP was much higher than that of GP or CP with induced time of about 180 s. Respectively, it was shown in the Fig.7 (H) ($k$(GPDAP)=2.146×10$^{-2}$ s$^{-1}$, $k$(GP)=1.550×10$^{-4}$ s$^{-1}$, $k$(CP)=6.553×10$^{-5}$ s$^{-1}$ and $k$(blank)=2.926×10$^{-5}$ s$^{-1}$). A summary of the constants for the catalytic actions in this paper was presented in Table 1. Compared with the results reported in other papers in Table s1, our catalysts showed higher catalytic activity. It can been seen from Fig.8 that the recovered catalysts still kept good catalytic activity for the reduction of 4-NP even after five circles in 9 min with a small decrease of conversion from 99% to 93%, which might owe to the loss of Pd. This result indicated the good stability of the catalyst which attributed to the strong interaction between PDA and Pd.

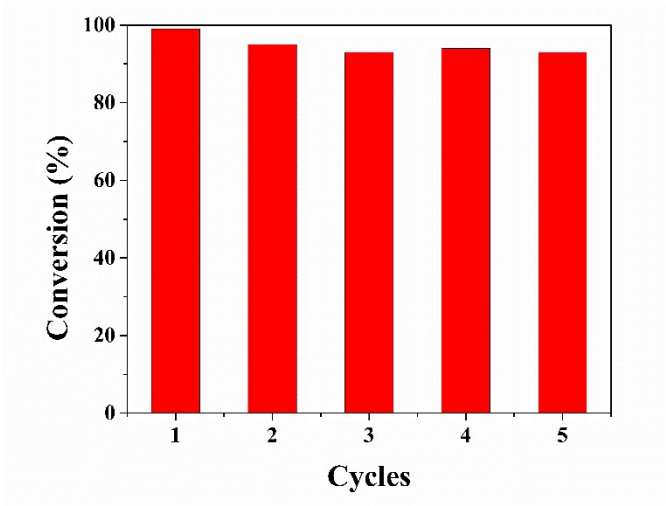


Fig. 8 Reusability of GPDAP for the reduction of 4-NP.

## 4 Conclusion

In conclusion, an ultrafine Pd catalyst propelled by the fantastic property of polydopamine had been successfully prepared through a facile method. The obtained catalyst possessed 2.0 nm of average size for Pd nanoparticles, and showed a good monodisipersity. This catalyst (GPDAP) was evaluated through catalyzing the reduction of 4-NP, $K_3[Fe(CN)_6]$, methylene blue (MB) and rhodamine B (RhB) which are common toxics in many fields and demonstrated much higher activity compared with GP and CP. Further applications for other catalysis are currently being processed and will be reported soon.

## References

1. J. Noh and R. Meijboom, in *Application of Nanotechnology in Water Research*, John Wiley & Sons, Inc., 2014, DOI: 10.1002/9781118939314.ch13, pp. 333-405.
2. Y. Wang, D. Zhao, W. Ma, C. Chen and J. Zhao, *Environ. Sci. Technol.*, 2008, 42, 6173-6178.
3. V. Mazumder and S. Sun, *J. Am. Chem. Soc.*, 2009, 131, 4588-4589.
4. R. Long, Z. Rao, K. Mao, Y. Li, C. Zhang, Q. Liu, C. Wang, Z.-Y. Li, X. Wu and Y. Xiong, *Angew. Chem.*, 2015, 127, 2455-2460.
5. N. Miyaura and A. Suzuki, *Chem. Rev.*, 1995, 95, 2457-2483.
6. Y. Gao, X. Ding, Z. Zheng, X. Cheng and Y. Peng, *Chem. Commun. (Camb.)*, 2007, DOI: 10.1039/b706490j, 3720-3722.
7. Z. Zhang, T. Sun, C. Chen, F. Xiao, Z. Gong and S. Wang, *ACS Appl. Mater. Interfaces*, 2014, 6, 21035-21040.
8. Z. Zhang, F. Xiao, J. Xi, T. Sun, S. Xiao, H. Wang, S. Wang and Y. Liu, *Sci. Rep.*, 2014, 4, 4053.
9. M. Heemeier, A. F. Carlsson, M. Naschitzki, M. Schmal, M Bäumer and H.-J. Freund, *Angew. Chem. Int. Ed.*, 2002, 41, 4073-4076.
10. D. Esken, X. Zhang, O. I. Lebedev, F. Schroder and R. A. Fischer, *J. Mater. Chem.*, 2009, 19, 1314-1319.
11. S. Royer, D. Duprez, F. Can, X. Courtois, C. Batiot-Dupeyrat, S. Laassiri and H. Alamdari, *Chem. Rev.*, 2014, 114, 1029-10368.
12. M. B. Gawande, P. S. Branco and R. S. Varma, *Chem. Soc. Rev.*, 2013, 42, 3371-3393.
13. M. Ayán-Varela, J. I. Paredes, L. Guardia, S. Villar-Rodil, J. M. Munuera, M. Díaz-González, C. Fernández-Sánchez, A. Martínez-Alonso and J. M. D. Tascón, *ACS Appl. Mater. Interfaces*, 2015, 7, 10293-10307.
14. K. S. Novoselov, A. K. Geim, S. V. Morozov, D. Jiang, Y. Zhang, S. V. Dubonos, I. V. Grigorieva and A. A. Firsov, *Science*, 2004, 306, 666-669.
15. S. Bae, H. Kim, Y. Lee, X. Xu, J.-S. Park, Y. Zheng, J. Balakrishnan, T. Lei, H. Ri Kim, Y. I. Song, Y.-J. Kim, K. S. Kim, B. Ozyilmaz, J.-H. Ahn, B. H. Hong and S. Iijima, *Nat Nano*, 2010, 5, 574-578.
16. S. Alwarappan, A. Erdem, C. Liu and C.-Z. Li, *J. Phys. Chem. C*, 2009, 113, 8853-8857.
17. G. Girishkumar, T. D. Hall, K. Vinodgopal and P. V. Kamat, *J. Phys. Chem. B*, 2005, 110, 107-114.
18. J. Pyun, *Angew. Chem. Int. Ed.*, 2011, 50, 46-48.
19. R. Ren, S. Li, J. Li, J. Ma, H. Liu and J. Ma, *Catal. Sci. Technol.*, 2015, 5, 2149-2156.
20. C. Ataca, E. Aktürk, S. Ciraci and H. Ustunel, *Appl. Phys. Lett.*, 2008, 93.
21. Y. Pan, H. Bao, N. G. Sahoo, T. Wu and L. Li, *Adv. Funct. Mater.*, 2011, 21, 2754-2763.
22. T. Zeng, X.-l. Zhang, Y.-r. Ma, H.-y. Niu and Y.-q. Cai, *J. Mater. Chem.*, 2012, 22, 18658-18663.
23. Y. Li, X. Fan, J. Qi, J. Ji, S. Wang, G. Zhang and F. Zhang, *Nano Research*, 2010, 3, 429-437.
24. D. V. Kosynkin, A. L. Higginbotham, A. Sinitskii, J. R. Lomeda, A. Dimiev, B. K. Price and J. M. Tour, *Nature*, 2009, 458, 872-876.
25. Y. Liu, J. Zhou, X. Zhang, Z. Liu, X. Wan, J. Tian, T. Wang and Y. Chen, *Carbon*, 2009, 47, 3113-3121.
26. X. Zhong, J. Jin, S. W. Li, Z. Y. Niu, W. Q. Hu, R. Li and J. T. Ma, *Chem. Commun.*, 2010, 46, 7340-7342.
27. X. Qi, K.-Y. Pu, H. Li, X. Zhou, S. Wu, Q.-L. Fan, B. Liu, F. Boey, W. Huang and H. Zhang, *Angew. Chem. Int. Ed.*, 2010, 49, 9426-9429.
28. S. W. Li, S. J. Guo, H. L. Yang, G. L. Gou, R. Ren, J. Li, Z. P. Dong, J. Jin and J. T. Ma, *J. Hazard. Mater.*, 2014, 270, 11-17.

29. Y. Xu, H. Bai, G. Lu, C. Li and G. Shi, *J. Am. Chem. Soc.*, 2008, 130, 5856-5857.
30. J. Liu, J. Tang and J. J. Gooding, *J. Mater. Chem.*, 2012, 22, 12435-12452.
31. J. H. WAITE and M. L. TANZER, *Science*, 1981, 212, 1038-1040.
32. H. Lee, S. M. Dellatore, W. M. Miller and P. B. Messersmith, *Science*, 2007, 318, 426-430.
33. H. Lee, N. F. Scherer and P. B. Messersmith, *Proc. Natl Acad. Sci.*, 2006, 103, 12999-13003.
34. L. Q. Xu, W. J. Yang, K.-G. Neoh, E.-T. Kang and G. D. Fu, *Macromolecules*, 2010, 43, 8336-8339.
35. W. Ye, X. Shi, J. Su, Y. Chen, J. Fu, X. Zhao, F. Zhou, C. Wang and D. Xue, *Appl. Catal. B- Environ.*, 2014, 160–161, 400-407.
36. W. Ye, Y. Chen, Y. Zhou, J. Fu, W. Wu, D. Gao, F. Zhou, C. Wang and D. Xue, *Electrochim. Acta*, 2014, 142, 18-24.
37. M. Zhao, C. Deng and X. Zhang, *ACS Appl. Mater. Interfaces*, 2013, 5, 13104-13112.
38. K. R. Paton, E. Varrla, C. Backes, R. J. Smith, U. Khan, A. O'Neill, C. Boland, M. Lotya, O. M. Istrate, P. King, T. Higgins, S. Barwich, P. May, P. Puczkarski, I. Ahmed, M. Moebius, H. Pettersson, E. Long, J. Coelho, S. E. O'Brien, E. K. McGuire, B. M. Sanchez, G. S. Duesberg, N. McEvoy, T. J. Pennycook, C. Downing, A. Crossley, V. Nicolosi and J. N. Coleman, *Nat Mater*, 2014, 13, 624-630.
39. P. Herves, M. Perez-Lorenzo, L. M. Liz-Marzan, J. Dzubiella, Y. Lu and M. Ballauff, *Chem. Soc. Rev.*, 2012, 41, 5577-5587.
40. M. A. White, J. A. Johnson, J. T. Koberstein and N. J. Turro, *J. Am. Chem. Soc.*, 2006, 128, 11356-11357.
41. L. Xu, J. Liao, L. Huang, D. Ou, Z. Guo, H. Zhang, C. Ge, N. Gu and J. Liu, *Thin Solid Films*, 2003, 434, 121-125.
42. A. Gupta, G. Chen, P. Joshi, S. Tadigadapa and Eklund, *Nano Lett.*, 2006, 6, 2667-2673.
43. B. Fei, B. Qian, Z. Yang, R. Wang, W. C. Liu, C. L. Mak and J. H. Xin, *Carbon*, 2008, 46, 1795-1797.
44. S. W. Li, H. L. Yang, Z. P. Dong, S. J. Guo, J. H. Zhao, G. L. Gou, R. Ren, J. W. Huang, J. Jin and J. T. Ma, *Catal. Sci. Technol.*, 2013, 3, 2303-2310.
45. B. E. Koel, A. Sellidj and M. T. Paffett, *Phys. Rev. B*, 1992, 46, 7846-7856.
46. M. Simões, S. Baranton and C. Coutanceau, *Appl. Catal. B-Environ.*, 2010, 93, 354-362.
47. M. Brun, A. Berthet and J. C. Bertolini, *J. Electron. Spectrosc. Relat. Phenom.*, 1999, 104, 55-60.
48. M. Schrinner, M. Ballauff, Y. Talmon, Y. Kauffmann, J. Thun, M. Möller and J. Breu, *Science*, 2009, 323, 617-620.
49. S. Carregal-Romero, J. Pérez-Juste, P. Hervés, L. M. Liz-Marzán and P. Mulvaney, *Langmuir*, 2009, 26, 1271-1277.
50. N. Pradhan, A. Pal and T. Pal, *Colloid Surf. A-Physicochem. Eng. Asp.*, 2002, 196, 247-257.
51. Y. Li, Q. Du, T. Liu, J. Sun, Y. Jiao, Y. Xia, L. Xia, Z. Wang, W. Zhang, K. Wang, H. Zhu and D. Wu, *Mater. Res. Bull.*, 2012, 47, 1898-1904.
52. X. Yang, X. Zhang, Y. Ma, Y. Huang, Y. Wang and Y. Chen, *J. Mater. Chem.*, 2009, 19, 2710-2714.
53. H.-U. Blaser, *Science*, 2006, 313, 312-313.
54. K. Esumi, R. Isono and T. Yoshimura, *Langmuir*, 2003, 20, 237-243.
55. C. Deraedt, L. Salmon, S. Gatard, R. Ciganda, R. Hernandez, J. Ruiz and D. Astruc, *Chem. Commun.*, 2014, 50, 14194-14196.
56. Y. Zhang, P. L. Zhu, L. Chen, G. Li, F. R. Zhou, D. Q. Lu, R. Sun, F. Zhou and C. P. Wong, *J Mater. Chem. A*, 2014, 2, 11966-11973.
57. L. Wang, Y. Zeng, A. Shen, X. Zhou and J. Hu, *Chem. Commun.*, 2015, 51, 2052-2055.
58. S. Wunder, F. Polzer, Y. Lu, Y. Mei and M. Ballauff, *J. Phys. Chem. C*, 2010, 114, 8814-8820.
59. X. Zhou, W. Xu, G. Liu, D. Panda and P. Chen, *J. Am. Chem Soc.*, 2009, 132, 138-146.
60. J. Zhang, Z. Xiong and X. S. Zhao, *J. Mater. Chem.*, 2011, 21 3634-3640.
61. Y. Li, G. Lu and S. Li, *J. Photochem. Photobiol. A Chem.*, 2002, 152, 219-228.

**Graphical Abstract**

# Well-dispersive graphene-polydopamine-Pd hybrid with enhanced catalytic performance

*Jian-Xin Ma, Honglei Yang, Shuwen Li, Ren Ren, Jing Li, Xueyao Zhang and Jiantai Ma**

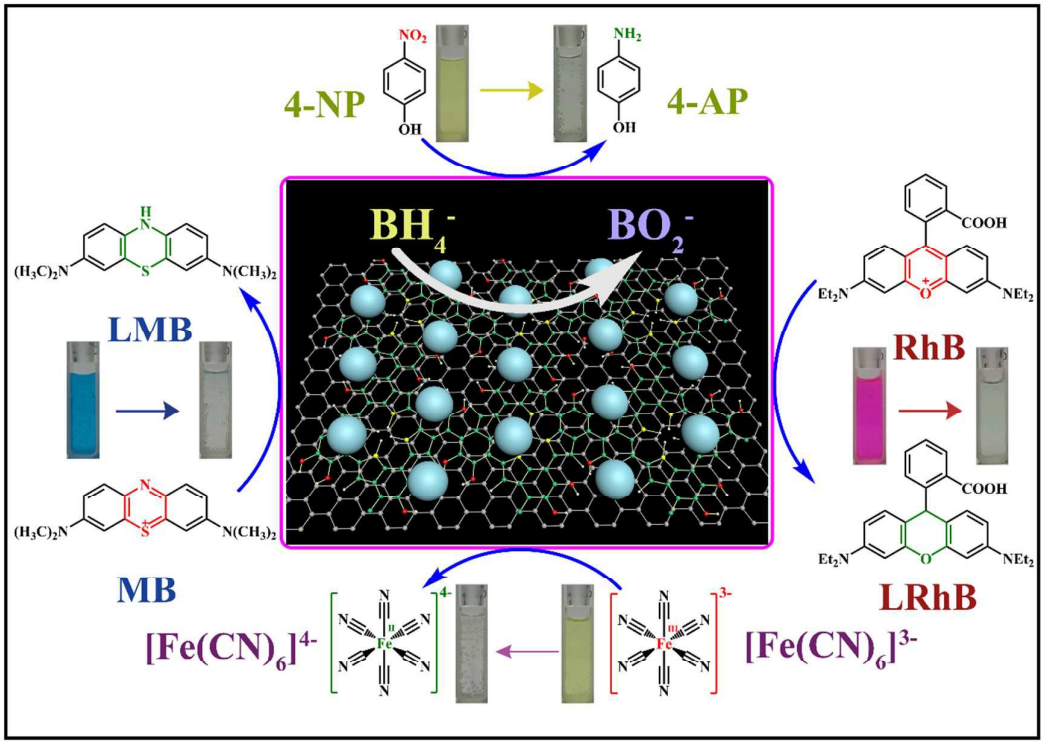


We reported a method to functionalize Graphene prepared by physical routes with polydopamine. Then a catalyst of ultrafine Pd nanoparticles which were stable and dispersed well in the polar solvents was prepared. The Pd nanoparticles were as small as 2.8 nm in average and had good monodispersibility in water by virtue of polydopamine modified graphene. In comparison with Palladium on carbon (CP) and Graphene-Pd (GP), the Pd nanoparticles dispersed with the help of polydopamine modified graphene (GPDAP) showed enhanced activity even with tiny amounts of catalysts added for the reduction of 4-nitrophenol (4-NP), $K_3[Fe(CN)_6]$, methylene blue (MB) and rhodamine B (RhB).